Targeting the tetraspanin CD81 reduces cancer invasion and metastasis

Felipe Vences-Catalán[a], Ranjani Rajapaksa[a], Chiung-Chi Kuo[a], Caitlyn L. Miller[b], Anderson Lee[a], Vishnu C. Ramani[c], Stefanie S. Jeffrey[c], Ronald Levy[a,1], and Shoshana Levy[a,1]

[a]Division of Oncology, Department of Medicine, Stanford University School of Medicine, Stanford, CA 94305; [b]Department of Bioengineering, Stanford University, Stanford, CA 94305; and [c]Department of Surgery, Stanford University School of Medicine, Stanford, CA 94305

Contributed by Ronald Levy, May 5, 2021 (sent for review September 8, 2020; reviewed by Stephen C. Blacklow, Natarajan Muthusamy, and Annemiek van Spriel)

Tetraspanins are an evolutionary conserved family of proteins involved in multiple aspects of cell physiology, including proliferation, migration and invasion, protein trafficking, and signal transduction; yet their detailed mechanism of action is unknown. Tetraspanins have no known natural ligands, but their engagement by antibodies has begun to reveal their role in cell biology. Studies of tetraspanin knockout mice and of germline mutations in humans have highlighted their role under normal and pathological conditions. Previously, we have shown that mice deficient in the tetraspanin CD81 developed fewer breast cancer metastases compared to their wild-type (WT) counterparts. Here, we show that a unique anti-human CD81 antibody (5A6) effectively halts invasion of triple-negative breast cancer (TNBC) cell lines. We demonstrate that 5A6 induces CD81 clustering at the cell membrane and we implicate JAM-A protein in the ability of this antibody to inhibit tumor cell invasion and migration. Furthermore, in a series of in vivo studies we demonstrate that this antibody inhibits metastases in xenograft models, as well as in syngeneic mice bearing a mouse tumor into which we knocked in the human CD81 epitope recognized by the 5A6 antibody.

immunotherapy | JAM-A | xenograft

CD81 belongs to the tetraspanin family of proteins (1). Tetraspanins form specialized membranal platforms known as tetraspanin-enriched microdomains (TEMs) (2). TEMs serve as scaffold structures facilitating the recruitment of their associated partner proteins, which in turn, contribute to a vast array of cellular processes (3). However, little is known about the consequences of these molecular interactions under normal or pathological conditions.

Recently the crystal structure of the complete CD81 protein was solved (4). It revealed that cholesterol is embedded in a cavity within the four transmembrane domains of the molecule. Molecular dynamic simulation showed that the presence or absence of cholesterol could shift the conformation of the large extracellular loop (LEL) of CD81 from an open to a closed conformation, respectively. In a subsequent study the crystal structure of the CD81-LEL complexed with the Fab fragment of 5A6 an anti-human CD81 monoclonal antibody (mAb) (5) was also solved (6). That study demonstrated that 5A6 engagement induces a conformational change in helices C and D in the LEL. In the current study we show that 5A6 is the only antibody that affected tumor cell invasion and metastasis of breast cancer cells.

The expression of CD81 in melanoma in humans was shown to promote tumor growth and metastasis (7), and knockdown of human CD81 in osteosarcoma and breast cancer cells reduced tumor progression and dissemination (8, 9). Moreover, mice deficient in CD81 developed fewer lung metastases when injected orthotopically with mouse breast cancer tumors (10). Furthermore, we recently demonstrated that 5A6 is unique among anti-CD81 mAbs in its ability to kill follicular lymphoma tumor cells while sparing normal lymphocytes (11).

Here we explore the role of CD81 in preclinical models of triple-negative breast cancer (TNBC). We demonstrate the exceptional property of 5A6 compared to other antibodies to cluster CD81 molecules and to inhibit breast cancer cell migration and invasion. Moreover, we implicate JAM-A, a tight junction protein, in the antimetastatic properties mediated by this antibody.

Results

5A6 Inhibits Invasion and Migration of Human Breast Cancer Cells In Vitro. Cell invasion and migration are processes that enable metastasis of tumor cells (12). Here we tested the effect of different anti-human CD81 mAbs on a human TNBC cell line, MDA-MB-231, in a three-dimensional (3D) spheroid invasion assay. MDA-MB-231 cells were seeded in sphere formation media to drive cell aggregation, followed by embedding the spheres in an invasion matrix composed of basement membrane proteins containing anti-human CD81 mAbs, including 5A6, 1D6, JS81, 1.3.3.22, or an isotype control mAb. All the anti-CD81 mAbs bound equally to the MDA-MB-231 and MDA-MB-436 cell lines, but only 5A6 completely abrogated cell invasion as shown in Fig. 1*A* and quantified in Fig. 1 *B* and *C*. In contrast, none of the other three anti-human CD81 mAbs inhibited cell invasion (Fig. 1 *A* and *B*). This unique ability of 5A6 to inhibit cell invasion was also observed in a human lung carcinoma cell line, A459 (*SI Appendix*, Fig. S1*A*).

Next, we tested whether 5A6 will inhibit cell migration. MDA-MB-231 cells migrate and adhere to the bottom chambers of Transwell inserts after 5 h, but in the presence of 5A6 very few cells were detected attached to the bottom of the well (Fig. 1*D*). Similarly, 5A6 but not any of the other anti-CD81 mAbs inhibited migration

Significance

CD81 belongs to the evolutionary conserved tetraspanin family of proteins that form specialized membranal platforms that facilitate a vast array of cellular processes. However, little is known about the consequences of these molecular interactions under normal or pathological conditions. Tetraspanins have no known natural ligands, but ligation by some antibodies induces functional consequences. Here we show that engagement of CD81 with 5A6 halts tumor invasion in vitro and reduces breast cancer metastasis in vivo. Altogether, these finding highlight the role of CD81 in cancer progression.

Author contributions: F.V.-C., R.R., C.-C.K., R.L., and S.L. designed research; F.V.-C., R.R., C.-C.K., C.L.M., A.L., and V.C.R. performed research; S.S.J. contributed new reagents/analytic tools; F.V.-C., R.R., C.-C.K., V.C.R., and S.L. analyzed data; and F.V.-C., R.L., and S.L. wrote the paper.

Reviewers: S.C.B., Harvard Medical School; N.M., The Ohio State University; and A.v.S., Radboud Institute for Molecular Life Sciences.

Competing interest statement: S.S.J. is an expert advisor for Ravel Biotechnology and Quantumcyte.

[1]To whom correspondence may be addressed. Email: levy@stanford.edu or slevy@stanford.edu.

This article contains supporting information online at https://www.pnas.org/lookup/suppl/doi:10.1073/pnas.2018961118/-/DCSupplemental.

Published June 7, 2021.

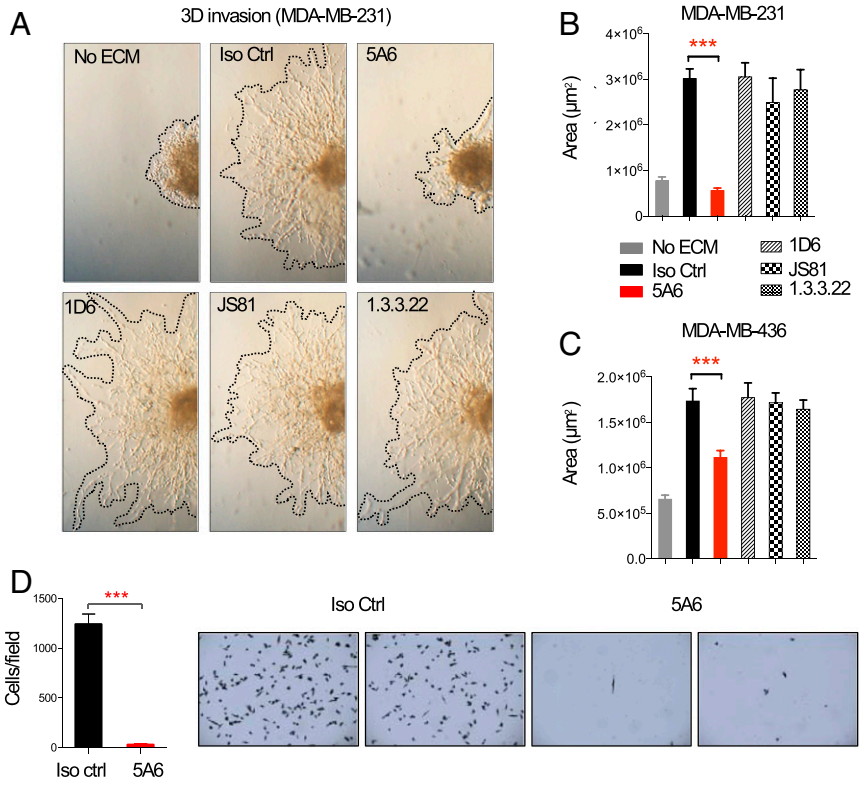

Fig. 1. Anti-human CD81 5A6 mAb inhibits human breast cancer invasion and migration in vitro. (*A* and *B*) 3×10^3 MDA-MB-231 or (*C*) MDA-MB-436 cells were seeded in a 96-well round-bottom plate in 1× spheroid formation ECM and incubated for 48 to 72 h to promote sphere formation. Then invasion matrix was added containing 10 μg/mL of anti-CD81 IgG1 mAbs (5A6, 1D6, JS81, or 1.3.3.22) or isotype control mAb. Photographs were taken at 72 h and invaded areas were analyzed using ImageJ software. Shown are mean ± SEM, Student's *t* test, $P = 0.0001$***. (*D*) 1×10^5 human MDA-MB-231 cells were starved in 0.1% FBS-containing RPMI media overnight. The next day cells were incubated with 10 μg/mL of mouse anti-human CD81 5A6 IgG1 or isotype control mAb before placing them on the top Transwell chamber. Cells that migrated after 5 h to the bottom chamber were quantified by crystal violet staining (*n* = three independent experiments). Shown are mean ± SEM, Student's *t* test, $P = 0.0002$***.

of MDA-MB-231 cells in an in vitro scratch assay (*SI Appendix*, Fig. S1*B*).

5A6 Induces Clustering of CD81 at the Cell Surface Membrane. Loss of cell-to-cell interaction is needed for tumor cells to acquire a metastatic phenotype, also known as epithelial–mesenchymal transition (EMT) (13). Interactions at tight junctions and focal adhesions serve as subcellular sites where signaling events occur. These site-specific localizations recruit signaling molecules and cluster proteins, including integrins, cell surface receptors, and tetraspanins (14). To explore the distribution of CD81 at the cell membrane in response to engagement by the anti-CD81 mAbs, we stimulated MDA-MB-231 cells with 5A6, 1D6, JS81, or 1.3.3.22 mAbs for 1 h at 37 °C. We also tested the distribution of CD81 under resting conditions by analyzing the binding of these antibodies to fixed cells. We then detected the distribution of CD81 by a goat anti-mouse-FITC antibody, followed by confocal microscopy analysis. In resting conditions, all the antibodies detected a similar diffuse distribution of CD81 on the cell membranes (Fig. 2*A*), but after 1 h of stimulation with 5A6, we observed clustering of CD81, as quantified (Fig. 2 *A* and *B*). By contrast, stimulation by 1D6, JS81, or 1.3.3.22, hardly clustered CD81 (Fig. 2*A* and *SI Appendix*, Fig. S2). Next, we found that CD81 colocalized with wheat germ agglutinin (WGA), a cell membrane marker in both stimulated and resting conditions, as determined by the Pearson's correlation coefficient (*SI Appendix*, Fig. S3). Moreover, a closer analysis revealed that CD81 redistributes at the cell-to-cell contact areas (Fig. 2*B*). This specific relocation of CD81 only by 5A6 is illustrated by line scans of protein density (Fig. 2 *C* and *D*).

JAM-A Is Required for Inhibition of Breast Cancer Invasion and Migration by 5A6. Junctional Adhesion Molecule A (JAM-A) is a transmembrane component of tight junctions, known to interact with different integrins and some tetraspanins (15). JAM-A expression was shown to correlate with the metastatic potential of different breast cancer cell lines (16). We, therefore, knocked out the *JAM-A* gene in MDA-MB-231 cells using CRISPR/Cas9 (Fig. 3*A*) and analyzed cell invasion in MDA-MB-231 JAM-A knockout (KO) cells. As expected, 5A6 inhibited invasion of parental cells (Fig. 3 *B*, *Left*), but in the absence of JAM-A, 5A6 inhibition was partially reversed (Fig. 3 *B*, *Right*). Similarly, a higher percentage of migrating MDA-MB-231 JAM-A KO cells were detected in the presence of 5A6, compared to parental cells in Transwell assays (Fig. 3*C*). To determine whether CD81 clusters locate to the tight junctions after 5A6 stimulation, we performed colocalization assays. A549 cells display a more epithelium-like phenotype retaining some epithelial characteristics such as tight junction formation, whereas MDA-MB-231 cells have a more mesenchymal-like phenotype with lower expression of these tight junction proteins, including JAM-A (16). We incubated a monolayer of A549 cells with 5A6 for 1 h or left the cells unstimulated. Cells were fixed and permeabilized and then stained for JAM-A or ZO-1, another tight junction marker, and analyzed by confocal microscopy. We found that 5A6 also induces CD81 clustering in A549 cells (Fig. 3*D*). Moreover, CD81 colocalized with JAM-A and ZO-1 and this colocalization significantly increased after 5A6 stimulation (Fig. 3*D*). However, we did not detect a direct physical interaction between CD81 and JAM-A. Interestingly, JAM-A has been shown to physically associate with the tetraspanin CD9 (15).

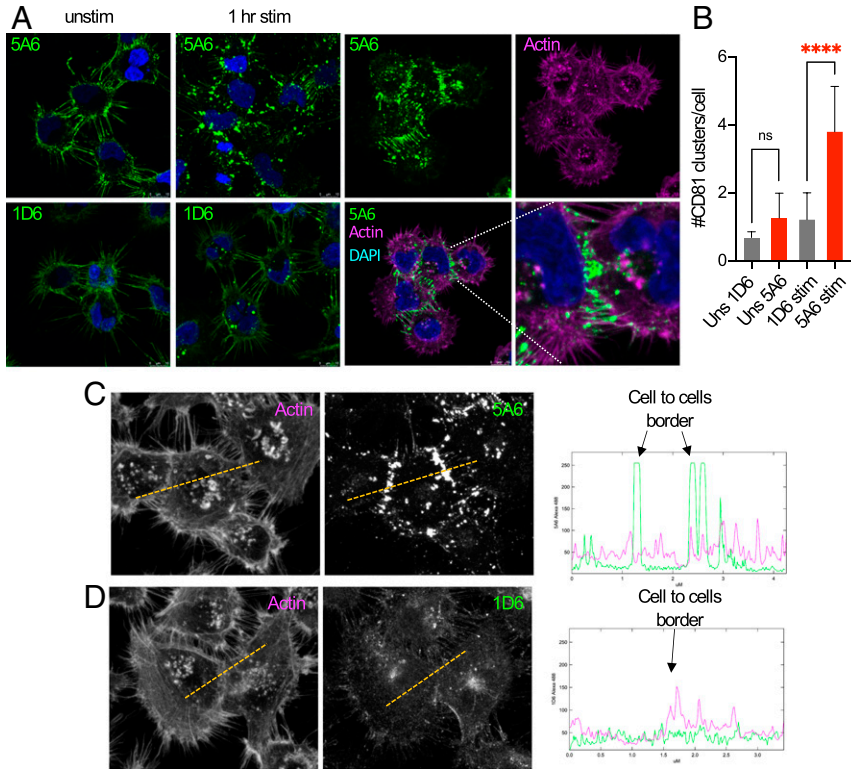

Fig. 2. 5A6 clusters CD81 preferentially at the cell-to-cell contact areas. (*A* and *B*) MDA-MB-231 cells were plated on fibronectin-coated coverslips and left unstimulated or incubated at 37 °C for 1 h (stim) with mouse IgG1 anti human CD81 5A6, or 1D6, as indicated. Unstimulated (unstim) cells were then fixed and permeabilized, followed by staining the indicated anti-CD81 mAbs. Stimulated and unstimulated cells were then stained with an anti-mouse IgG1 FITC-conjugated secondary antibody and with phalloidin-Alexa-647 to stain the actin cytoskeleton. Coverslips were mounted in ProGold media with DAPI and analyzed by confocal microscopy (photos were taken at 63× magnification). (*B*) Shown is the number of CD81 clusters per cell. Arbitrary defined thresholds for CD81 clusters were quantified using ImageJ. (*C* and *D*) Line scans through adjacent cells plot phalloidin (actin)-Alexa 647, 5A6 (*C*), or 1D6 (*D*) Alexa-488 density. (n = three independent experiments). Shown are mean ± SD, Student's t test, $P = 0.0001$****. ns, not significant.

In addition, staurosporine, which inhibits several kinases, significantly reversed the inhibitory effect of 5A6 on cell invasion (*SI Appendix*, Fig. S4*A*). By contrast, chemical inhibition of several other protein kinases known to affect cell signaling pathways involved in cell invasion and migration such as PI3K (Wortmannin and LY294002), MEK1/2 (U0126), Rac1 (NSC23766), and integrins (RGDS peptide) had no significant effect on 5A6 invasion inhibition (*SI Appendix*, Fig. S4*B*).

5A6 Is Effective In Vivo against an Aggressive Human Breast Cancer Tumor. To test the therapeutic potential of 5A6 against progression of human breast cancer tumors, we orthotopically injected luciferase-expressing MDA-MB-231-luc cells, into the mammary fat pad of severe combined immunodeficient (SCID-beige) female mice. On day 5, postimplantation, tumor-bearing mice were injected intraperitoneally (i.p.) with mouse anti-human CD81 mAbs 5A6 IgG1 (Msγ1), a class-switched version of 5A6 IgG2a (Msγ2a), or isotype control as shown in Fig. 4*A*. Mice treated with 5A6 Msγ2a, which was superior in eliminating B cell lymphoma (11), effectively delayed primary tumor growth (Fig. 4 *B*, *Right*). By contrast, 5A6 Msγ1 had no effect on primary tumor growth compared to isotype control-treated mice (Fig. 4 *B*, *Middle*). Nevertheless, both 5A6 Msγ1 and Msγ2a effectively reduced spontaneous metastases to the lungs, liver, and spleen (Fig. 4*C*).

Previously, we demonstrated the superiority of 5A6 Msγ2a against B cell lymphoma in vivo by enhancing the activation of innate immune effectors, such as complement and antibody-dependent cell cytotoxicity (ADCC) (11). To determine whether the efficacy of 5A6 against breast cancer in vivo also involves such secondary immune mechanisms, we tested the ability of 5A6 Msγ2a to mediate ADCC in vitro. We incubated MDA-MB-231 cells with purified human natural killer (NK) cells in the presence of 5A6. Indeed, 5A6 Msγ2a mediated ADCC in the presence of NK cells (Fig. 4*D*).

5A6 Is Effective against a Patient-Derived TNBC Xenograft. Next, we tested the therapeutic effect of 5A6 against an aggressive patient-derived orthotopic xenograft (PDOX) breast cancer tumor. This PDOX model (SUTI151) was recently described in detail (17–19). This tumor expresses CD81 and EpCAM (Fig. 4*E*). A suspension of the patient's tumor cells embedded in Matrigel was injected into the mammary fat pad of SCID female mice, followed by weekly treatments with 5A6 Msγ2a or an isotype control antibody. 5A6 significantly reduced the growth of the PDOX tumor (Fig. 4*F*). Circulating tumor cells (CTCs), which were detected by reactivity with an anti-human EpCAM antibody and with a different anti-human CD81 mAb (JS81) that competes with 5A6 (20), were less than 50 CTCs/mL in all four 5A6-treated mice, but numerous in three out of four isotype control-treated mice (Fig. 4*G*).

Knockout of CD81 in a Mouse Triple-Negative Breast Cancer Delays Tumor Growth and Metastases. Expression of CD81 in human tumors was shown to promote metastasis in melanoma, osteosarcoma, and breast cancer (7–9). To evaluate the tumor-intrinsic role of CD81 in metastasis, we used CRISPR/Cas9 to knock out the *cd81* gene in the 4T1-luc TNBC cell line. Loss of CD81 expression was confirmed by flow cytometry and Western blot (Fig. 5*A*). We then compared tumor growth of parental and CD81KO 4T1-luc cells implanted orthotopically into the mammary fat pad of female Balb/c wild-type (WT) mice. Tumor growth was delayed in mice

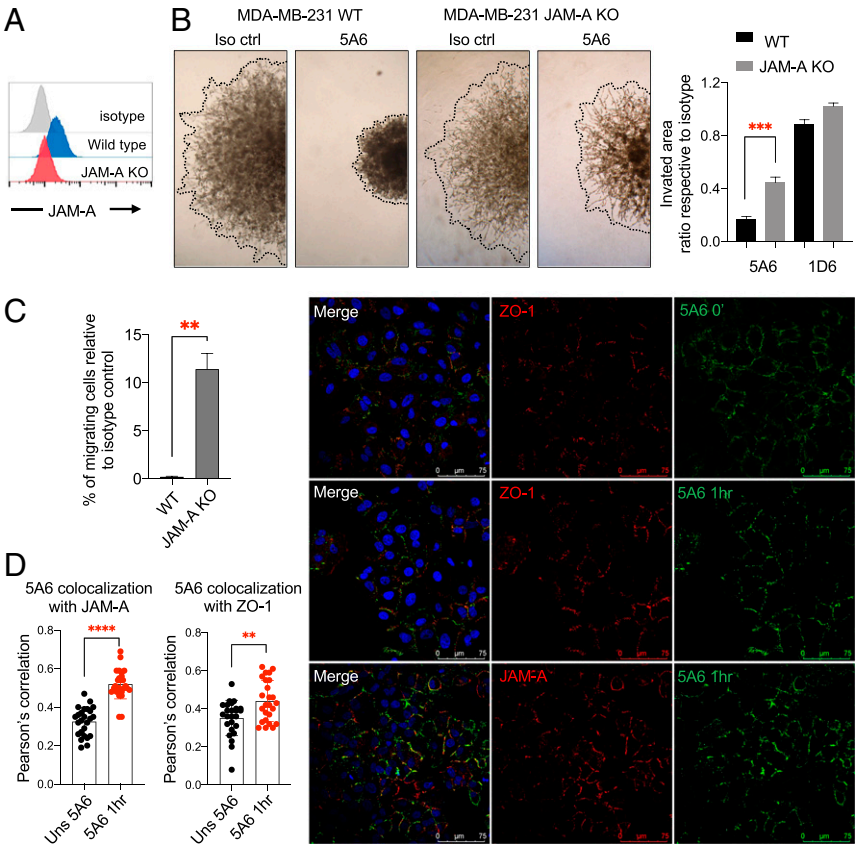

Fig. 3. JAM-A plays a role in 5A6-induced inhibition of invasion and migration. (*A*) Flow cytometry analysis of JAM-A cell surface expression on parental MDA-MB-231 and on JAM-A CRISPR/Cas9 knocked out cells. (*B*) The 3D spheroid invasion assay (done as in Fig. 1*A*), 3×10^3 parental MDA-MB-231 or JAM-A KO cells were incubated with the indicated antibodies. Photographs were taken at 96 h and invaded areas were analyzed using ImageJ software. Shown are mean ± SEM of the ratio respective their own isotype, Student's *t* test, $P = 0.0001$***. (*C*) Transwell migration assay of parental MDA-MB-231 or MDA-MB-231 JAM-A KO cells treated with isotype control or 5A6 mAb for 24 h and quantified by crystal violet staining. Shown is the percentage of migrating cells compared to their own isotype control. Shown are mean ± SEM, Student's *t* test, $P = 0.0024$** (two independent experiments done in triplicates). (*D*) A549 cells were plated on fibronectin-coated coverslips, left unstimulated, or incubated with mouse anti-human CD81 5A6-Alexa 488 at 37 °C for 1 h (stim) and then fixed. Unstimulated cells were fixed then stained with CD81 5A6-Alexa 488. Both fixed stimulated and unstimulated cells were also stained with rabbit anti-ZO-1 or JAM-A antibodies followed by anti-rabbit-Cy3 secondary antibody. Coverslips were mounted in ProGold media with DAPI and analyzed by confocal microscopy. (photos were taken at 40× magnification). Pearson's correlation between ZO-1 or JAM-A with 5A6 was calculated using ImageJ software (two independent experiments). Shown are mean ± SD, Student's *t* test, $P = 0.0029$**, $P = 0.0001$****.

injected with 4T1-luc CD81KO cells compared to 4T1-luc parental cells (Fig. 5 *B*, *Left*). Moreover, spontaneous lung metastases were significantly reduced (Fig. 5 *B*, *Right*). These results suggest that CD81 plays an important tumor-intrinsic role in tumor growth and metastasis.

An Anti-Mouse CD81 Antibody Inhibits Migration In Vitro and Reduces Experimental Breast Cancer Tumor Metastasis In Vivo. CD81 knockout mice develop fewer metastases when injected with the parental 4T1 mouse breast cancer tumor (10). To determine if an anti-mouse CD81 mAb could affect the motility of 4T1 cells, we seeded cells at the top of Transwells in the presence of an anti-mouse CD81 mAb, followed by quantifying the number of migrating cells that adhered to the bottom chambers. We found that the anti-mouse CD81 mAb, inhibited 4T1 cell migration (Fig. 6*A*). Next, we tested the effect of the antibody in an experimental model of metastasis in vivo. We treated WT Balb/c mice i.p. with the anti-CD81 mAb 1 d prior to intravenous (i.v.) injection of 4T1-luciferase-tagged parental cells (4T1-luc) and on days +1 and +3 after tumor injection (Fig. 6*B*). The anti-mouse CD81-treated group had significantly fewer lung metastases when compared to the vehicle control as evident by in vivo bioluminescence (IVIS Spectrum) and by enumeration of lung metastatic nodules (Fig. 6*C*).

Generation of 5A6 Epitope Knockin 4T1 (4T1-luc^{5A6KI}) Cells. Finally, to test the therapeutic effect of 5A6 in an immunocompetent mouse we knocked in the 5A6 epitope into 4T1-luc cells. We previously mapped the 5A6 epitope to the LEL of human CD81 (21), and more recently the 5A6 crystal structure bound to CD81 was described in more detail (6); briefly it demonstrated that the variable regions of both heavy and light chains engage key amino acids located at the LEL loop encoded on exons 6 and 7 of the *CD81* gene. We therefore replaced mouse exons 6/7, which contain the most variable region between mouse and human CD81 (*SI Appendix*, Fig. S5*A*) by using CRISPR/Cas9 and a donor template containing human CD81 exons 6/7 flanked by mouse homology arms to generate 4T1-luc^{5A6KI} (*SI Appendix*, Fig. S5*B*). Indeed, 5A6 binds to 4T1-luc^{5A6KI}, whereas an anti-mouse CD81 (Eat2) no longer binds the 4T1-luc^{5A6KI} cells as compared to parental cells (Fig. 7*A*). Moreover, the migration of these 4T1-luc^{5A6KI} cells was inhibited by 5A6 (Fig. 7*B*).

5A6 Reduces Metastasis in the 5A6 Epitope Knock in (4T1-luc^{5A6KI}) Breast Tumor in a Syngeneic Host. 5A6 Msγ2a was more effective than 5A6 MsγG1 against human breast cancer (Fig. 4). We therefore tested the effect of 5A6 Msγ2a against the newly generated 4T1-luc^{5A6KI} using the experimental model of metastasis in a syngeneic host. Tumor-bearing WT Balb/c mice were treated with 5A6

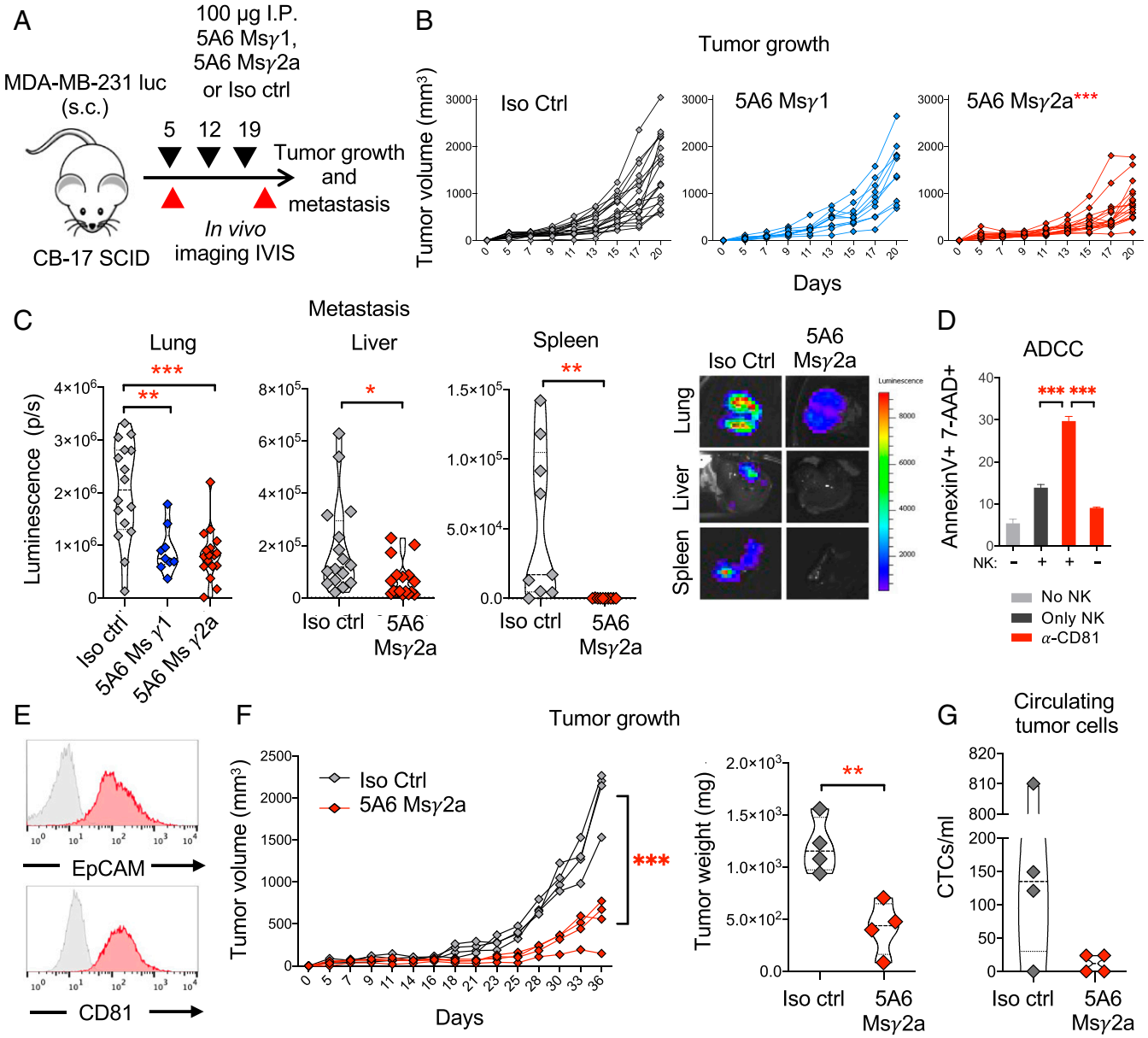

Fig. 4. Anti-human CD81 5A6 inhibits human breast cancer metastasis in vivo. (*A*) Schema: 1×10^5 MDA-MB-231-luc cells embedded in Matrigel 1:1 (vol/vol) were injected subcutaneously into the mammary fat pad of female SCID mice. On day 5 posttumor challenge, mice were injected with 100 µg of anti-CD81 5A6 MsIgG2a, 5A6 MsIgG1, or an isotype control mAb intraperitoneally and weekly thereafter for 2 more weeks. Tumor (*B*) growth was measured at the indicated points by caliper measurements and (*C*) organ metastasis (lung, liver, and spleen) was quantified ex vivo by bioluminescence (IVIS imaging) on day 20 (two independent experiments $n = 18$ in each group). (*D*) Analysis of ADCC. MDA-MB-231 cells were incubated in the presence or absence of human purified NK cells and 1 µg/mL of anti-human CD81 (5A6), followed by overnight incubation at 37 °C. Cell death was measured by staining with annexin-V and 7-AAD and analyzed by flow cytometry. Shown are mean ± SEM, Student's *t* test, $P = 0.0005$***. (*E*) A TNBC PDX expresses CD81 and EpCAM (red histograms) as analyzed by flow cytometry (gray histogram; isotype control). (*F*) 1×10^6 PDX cell suspensions were injected with Matrigel 1:1 (vol:vol) into the mammary fat pad of SCID mice subcutaneously. On day 9, mice were injected with 100 µg of anti-CD81 5A6 (MsIgG2a) or isotype control intraperitoneally and weekly thereafter for 3 more weeks. Tumor growth was measured by (*Left*) caliper at the indicated times and (*Right*) tumor weigh at endpoint (one single experiment, $n = 4$ in each group). (*G*) Circulating tumor cells were detected by positive staining of human EpCAM and human CD81 by flow cytometry. Shown are individual tumor measurements, two-way ANOVA comparing treatments, $P = 0.0001$***, Student's *t* test, $P = 0.0054$**, $P = 0.0139$*.

Msγ2a or an isotype control antibody, as illustrated in Fig. 7*C*. Mice were imaged on day 16, then killed, and ex-vivo lung metastasis was also quantified by bioluminescence (IVIS imaging). As evident in Fig. 7*D*, 5A6 greatly reduced metastasis to the lungs, reinforcing the in vivo antimetastatic properties of 5A6.

Discussion

The full human CD81 crystal structure reveals that the transmembrane domains consist of a separated pair of antiparallel helices, containing a cholesterol binding pocket (4). Furthermore, the 3D structure of a 5A6 Fab bound to CD81-LEL was also solved (6). It shows that both variable regions of the heavy and light chains of the 5A6 Fab bind to helices C and D in the CD81-LEL and shift both helices. While other anti-CD81 mAbs studied by Susa et al. and Nelson et al. also caused a shift in the 3D structure of the CD81-LEL helices, our results indicate that only 5A6 has the functional consequences on tumor cell invasion and metastases (6, 22). We therefore hypothesize that 5A6 uniquely disrupts the association of CD81 with a yet to be identified partner protein. Supporting this hypothesis are the most recent 3D structures of two

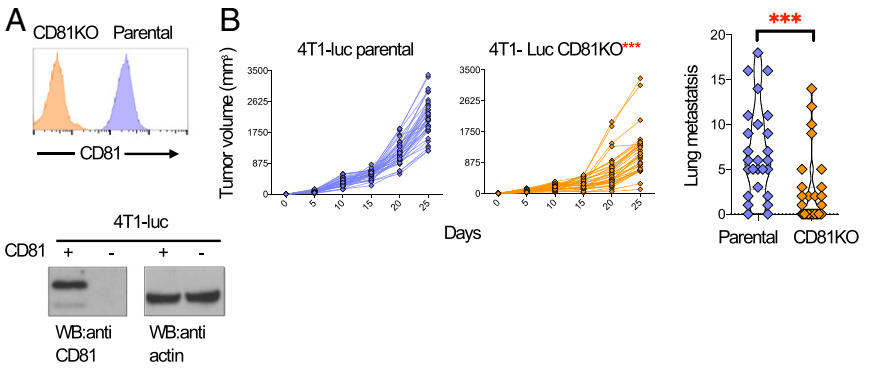

Fig. 5. Reduced tumor growth and metastasis in mice injected with a CD81-deficient mouse breast cancer tumor. (*A*) Analysis of 4T1-luc cells in which CD81 was knocked out by CRISPR/Cas9. Cell surface expression of 4T1-luc parental and CD81KO cells were assessed by flow cytometry (*Top*) and by Western blot (*Bottom*), actin served as a loading control. (*B*) 1×10^4 4T1-luc parental or CD81KO cells were injected subcutaneously into wild-type Balb/c mice. Tumor growth (*Left*) was monitored by caliper measurements at the indicated time points and lung metastases (*Right*) were measured by India ink staining. ($n = 35$ mice in each group, three independent experiments). Shown are individual mouse tumor measurements (*Left*), two-way ANOVA comparing treatments, $P = 0.0001$***, shown is mean ±SEM (*Right*), Student's *t*test, $P = 0.0004$**.

tetraspanins, CD81 and CD9, bound to their cell type-specific partner protein ectodomains (23, 24). In both cases, the 3D structures of both CD81 and CD9 changed their conformation when bound to their respective partner proteins. We speculate that engagement by 5A6, but not by other anti-CD81 mAbs, affects these partnerships, resulting in the observed functional consequence.

Tetraspanins such as CD9, CD37, CD81, CD82, and CD151 have long been implicated in cancer progression, but more recently, they have reemerged as candidate therapeutic targets against cancer (25, 26). CD81, one of the most studied tetraspanins, has been especially associated with malignant cellular transformation (27). It has been shown that down-regulation of CD81 in several cancers is associated with reduced tumor growth, migration, and cell invasion (8, 28, 29), and overexpression of CD81 in melanoma, increases metastasis (7). Here, we knocked out CD81 in a triple-negative mouse breast cancer, which resulted in reduced tumor growth and less metastasis, confirming the importance of CD81 during cancer progression.

Previously, we demonstrated that the anti-human CD81 mAb 5A6 effectively eliminated B cell lymphoma tumors, prolonging survival in mouse preclinical models (11). This result encouraged us to test our unique 5A6 mAb in solid tumors such as breast cancer. We find that this antibody is also effective against human TNBC tumors, and importantly it halts metastasis to multiple different organs. This antimetastatic effect was observed in a spontaneous as well as in an experimental model of metastasis and across different tumor models.

Cell migration and invasion are initial steps required for tumor cells to metastasize (30). These processes are tightly regulated by different proteins, including tetraspanins (25) and especially CD81 (27). Here, we showed that 5A6 inhibits cell migration and invasion of several breast cancer cell lines, suggesting that this antibody interferes with tumor dissemination by possibly restricting cell motility. Cell motility requires the interplay of different signaling pathways. Tetraspanins and integrins are known membrane proteins that mediate cell migration and adhesion by interacting with the extracellular matrix and recruiting signaling molecules (3). Our observation that only 5A6 induces clustering of CD81 at the cell-to-cell contact areas, suggests that this antibody interferes with cell interactions. Expression of JAM-A, a component of tight junctions, was previously shown to correlate with the invasion ability of breast cancer cell lines favoring more stable focal adhesions and

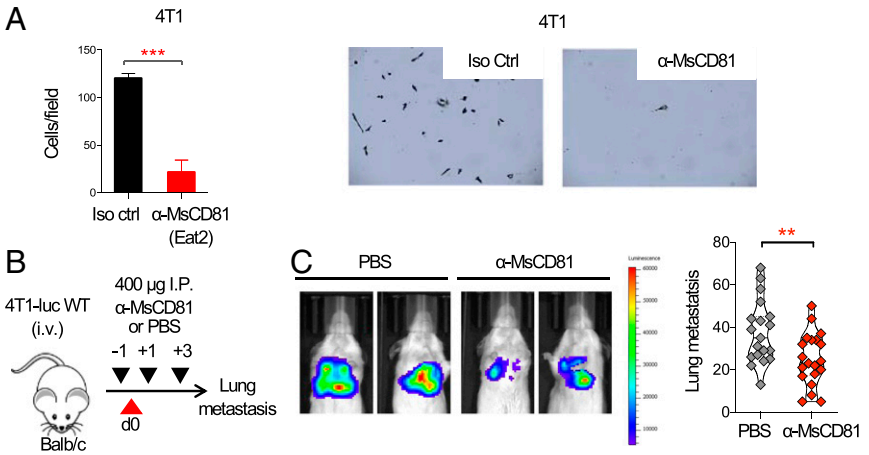

Fig. 6. An anti-mouse CD81 antibody inhibits breast cancer migration in vitro and reduces metastasis in vivo. (*A*) 4T1-luc cells were place at the top chamber in a Transwell assay and incubated with the indicated anti-mouse CD81 mAb (α-MsCD81) and its respective isotype control. Migrating cells attached at the bottom well were stained with crystal violet and quantified. Representative migrated cells are shown. Shown are mean ± SEM, Student's *t* test, $P = 0.0001$***. (*B*) Schema: Mice were injected with 400 µg of anti-mouse CD81 on day −1 and with 400 µg on days +1 and +3; on day 0 mice were injected with 2.5×10^4 4T1-luc intravenously; on day 16 mice were killed and lung metastasis was visualized (*C*, *Left*) by bioluminescence (IVIS imaging) and quantified (*C*, *Right*) by India ink staining ($n = 20$ mice in each group, three independent experiments). Shown are individual mouse metastatic nodule counts, Student's *t* test, $P = 0.0065$**.

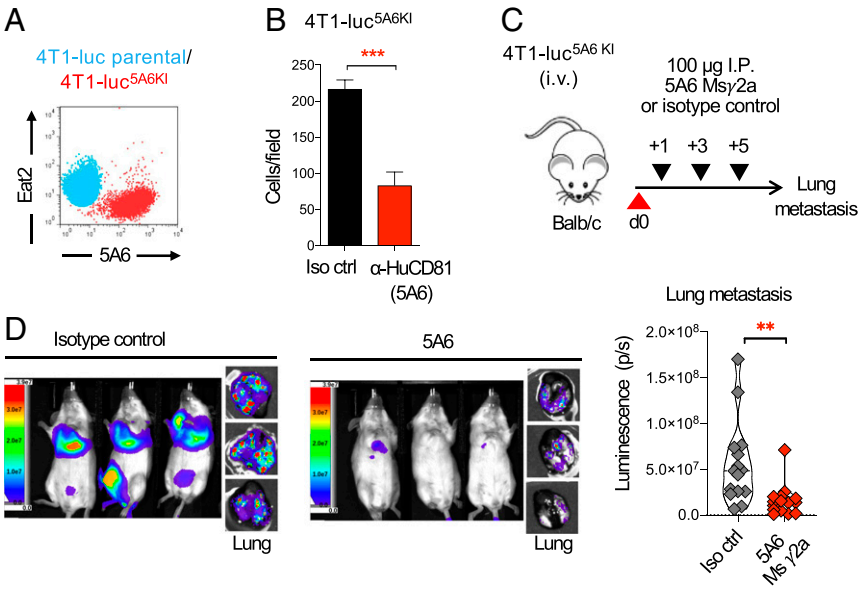

Fig. 7. 5A6 inhibits metastasis of the epitope knockin mouse breast cancer tumor 4T1-luc in a syngeneic mouse. (*A*) Flow cytometry analysis of Eat2 and 5A6 binding on parental 4T1-luc or 4T1-luc^{5A6KI}, the 5A6 epitope KI cell line. (*B*) 4T1-luc^{5A6KI} cells were placed at the top chamber of a Transwell assay and incubated with 5A6 or isotype control mAb; migrating cells attached at the bottom well were stained with crystal violet and quantified. Shown are mean ± SEM, Student's *t* test, $P = 0.0001$***. (*C*) Schema: Mice were injected intravenously with 2.5×10^4 4T1-luc^{5A6KI}, followed by treatment on days +1, +3, and +5 with 100 µg of 5A6 MsIgG2a or an isotype control. Full body images were analyzed on day 16, then mice were killed, and lung metastases were analyzed ex vivo by (*D*) bioluminescence (IVIS imaging). Median is shown. Student's *t* test, $P = 0.0035$** (two independent experiments, $n = 15$ in each group).

the establishment of functional tight junctions (16). In the absence of JAM-A, inhibition of invasion and migration by 5A6 was partially reversed, suggesting that clustering of CD81 especially at JAM-A- and ZO-1-containing areas might contribute to stabilizing cell interactions, therefore inhibiting the cell invasive behavior.

Staurosporine, a general kinase inhibitor, resulted in reduced 5A6 invasion inhibition. A known target of staurosporine is PKC. Indeed, PKC association with tetraspanins, including CD81 and integrins, has been reported (31). However, the specific PKC inhibitors, Gö-6976 and Gö-6983 (32), did not affect 5A6-induced inhibition of invasion and migration. Relatedly, 5A6 inhibited invasion and migration of MDA-MB-231 PKCα KO, and MDA-MB-231 PKCβ KO cells (*SI Appendix*, Fig. S4*C*). Similarly, chemical inhibition of PI-3K, MEK1/2, and Rac1 and a broad integrin inhibitor (RGDS peptide) did not impair the ability of 5A6 to inhibit cell invasion.

In addition to the intrinsic effect of 5A6 in inhibiting migration and invasion of breast cancer tumors, antibody therapy relies often on its ability to engage the immune system through an Fc-dependent manner. When 5A6 (mouse IgGγ1) was used as therapy, only metastasis but not tumor growth was reduced, but by class switching to mouse IgG2a, a more potent isotype known to mediate ADCC, not only metastasis but tumor growth was also reduced. These results indicate that in vivo, 5A6 inhibits tumor progression by a combination of different mechanisms.

In summary, we present here evidence for a cell intrinsic role of the tetraspanin CD81 on breast cancer tumor growth, invasion, and metastasis and a unique antibody 5A6 with antimetastatic properties that target the human CD81. 5A6 reduces metastasis and tumor growth in vivo both by inhibiting migration and invasion and by engaging the innate immune system. These results provide the rationale for further studies planned to determine both the safety and the efficacy of 5A6 in a model where both the tumor and the host express the human CD81 target.

Methods

Antibodies. Hamster anti-mouse Eat1, Eat2 (33), and mouse anti-human CD81 5A6 (5) and 1D6 (34) mAbs, were produced in house. Production and purification of 5A6 IgG1 and IgG2a (11) was outsourced (BioXCell). Mouse anti-human JS81 and 1.3.3.22 were purchased (BD Pharmingen and Santa Cruz Biotechnology, respectively) and goat anti-mouse IgG fluorescein isothiocyanate (FITC)-conjugated and goat anti-rabbit Cy3 were purchased from Southern Biotech. Anti-JAM-A antibody and wheat germ agglutinin-Alexa 647 were purchased from Thermo Fisher Scientific and anti-ZO-1 from Cell Signaling Technology.

Cell Lines and Generation of CD81KO and 5A6 Epitope Knockin Cell Lines. 4T1-luc (obtained from C. Contag, Stanford University, Stanford, CA), MDA-MB-231-luc (Cell Biolabs), and MDA-MB-436 (ATCC HTB-130) cells were maintained in RPMI medium and A549 cells (obtained from B. I. Sikic, Stanford University, Stanford, CA) in Dulbecco's Modified Eagle Medium containing 10% (vol/vol) fetal calf serum (FCS) (HyClone), 1% sodium pyruvate, 1% L-glutamine (Cellgro), 100 U/mL penicillin, and 100 µg/mL streptomycin (Gibco). 4T1-luc cells were transiently transfected using Lipofectamine 2000 with a pSpCas9(BB)-2A-GFP (pX458) (Addgene) plasmid containing sgRNA sequences targeting exon 2 of the *Cd81* gene (gRNA 5′ GCTGGCTGGAGGCGTGATCC 3′). CD81 knockout was verified by flow cytometry and Western blot. To knock out JAM-A from MDA-MB-231 we used sgRNAs 5′ CCCAACTCACGATTATTCTC 3′. To generate 5A6-epitope knockin cells (4T1-luc^{5A6KI}), 4T1-luc cells were cotransfected with a pSpCas9(BB)-2A-GFP (pX458) (Addgene) plasmid containing sgRNA sequences targeting the upstream region of exon 6 (5′ GCTGTCATTATGGTAAGCAC 3′), the downstream region of exon 7 of the mouse *Cd81* gene (5′ GCCACAACAGTTGAGCTGCA 3′), and the pENTR-donor plasmid containing human exons 6/7 flanked by 500 bp of the mouse homology arms. 4T1-luc CD81KO and 4T1-luc^{5A6KI} cells were selected by fluorescence active cell sorting after 24 to 48 h of transfection based on GFP expression and subsequently by two more rounds of sorting based on CD81 expression detected by lack of binding of anti-mouse CD81 Eat2 for 4T1-luc CD81KO cells or binding by anti-human CD81 5A6 for 4T1-luc^{5A6KI}.

Mouse Models. The 6- to 8-wk-old female Balb/c and SCID-beige mice were purchased from Charles River and housed at the pathogen-free animal facility of the Stanford University Medical Center. The syngeneic tumor model: 1×10^4 4T1-luc or 4T1-luc CD81KO cells were injected orthotopically into the mammary fat pad of Balb/c mice, tumor growth was monitored by caliper measurements every other day, and lung metastases were quantified after India ink staining.

For the syngeneic experimental model testing the effect of antibodies on metastasis, 2.5×10^4 4T1-luc cells were injected i.v. into female WT Balb/c mice and then treated i.p. with 400 µg of anti-mouse CD81 antibody a day prior to tumor challenge, and then on days 1+ and 3+. For the metastatic

model testing the effects of the anti-human CD81 5A6 antibody, we injected female Balb/c i.v. with 2.5×10^4 4T1-luc^{5A6KI} cells followed by treatment with 100 μg of 5A6 or isotype-matched igG2a control antibody 1 d after tumor injection and every other day for two more doses. Metastases were visualized by IVIS imaging and quantified by India ink staining. For xenograft models, 1×10^5 MDA-MB-231-luc cells or a suspension of 1×10^6 patient-derived xenograft (PDX151) (17) embedded in 50/50 vol/vol in Matrigel were injected orthotopically into the mammary fat pad of SCID mice. On day 5, mice were treated as detailed in the figure legends. Tumor growth was monitored by caliper measurements and by weighing of the excised tumors. Blood was collected by cardiac puncture and CTCs were quantified by flow cytometry using the anti-human CD81 mAb (JS81) and anti-EpCAM.

Transwell and 3D Invasion Assays. The 1×10^5 4T1, 4T1-luc^{5A6KI}, human MDA-MB-231, or MDA-MB-231 JAM-A KO cells were starved overnight in medium containing 0.1% fetal calf serum, then seeded at the top chamber of Transwell inserts in the presence of anti-CD81 mAbs or an isotype control antibody as indicated. After incubating MDA-MB-231 for 5 h or 4T1 or 4T1-luc^{5A6KI} for 24 h, cells migrating to the bottom of the well were quantified by crystal violet staining. The 3D invasion assays followed the manufacturer's specifications (Cultrex). Briefly, 3×10^3 MDA-MB-231, MDA-MB-231 JAM-A KO, MDA-MB-436, or A549 cells were seeded in an ultra-low binding 96-well plate with 10× spheroid formation extracellular matrix (ECM) to form cell spheroids for 1 to 3 d. Cells were then embedded in invasion matrix in the absence or presence of the indicated anti-CD81 or isotype control mAbs, or in the presence of dimethyl sulfoxide or the indicated protein inhibitors. The invasion area was quantified at 72 to 96 h using ImageJ software.

ADCC Assays. Human NK cells were purified using MACS kit (130-092-657), then cocultured at 5:1 effector:target ratio with carboxyfluorescein diacetate succinimidyl ester-labeled MDA-MB-231 cells for 24 h in the presence of 1 μg/mL of 5A6 mAb. Cell death was measured by staining with Annexin-V and 7-aminoactinomycin D (7-AAD) and analyzed by flow cytometry (BD LSR II).

Confocal Microscopy. MDA-MB-231 cells were plated on fibronectin-coated coverslips (BioCoat, Corning) and incubated at 37 °C with 10 μg/mL of mouse anti-human CD81 IgG1 mAbs 5A6, 1D6, JS81, or isotype control for 1 h. Cells were then fixed and permeabilized, followed by goat anti-mouse IgGs FITC secondary antibody and by phalloidin-Alexa 647 to stain the actin cytoskeleton. Coverslips were mounted in ProGold media with DAPI (Life Technologies) and analyzed in a SP8 confocal microscope; photos were taken with a 40× and 63× objective. Line scans and cluster quantification were analyzed using ImageJ software.

Colocalization Assays. MDA-MB-231 and A549 cells were plated on fibronectin-coated coverslips (BioCoat, Corning) and left unstimulated or incubated at 37 °C with 10 μg/mL of mouse anti-human CD81 5A6 mAb-Alexa 488 conjugated. Cells were then fixed and stained with rabbit anti-JAM-A, anti-Z0-1 antibodies followed by an anti-rabbit-Cy3-labeled secondary antibody or stained with the cell surface marker WGA-Alexa 647 labeled. Coverslips were then mounted in ProGold media with DAPI (Life Technologies) and analyzed in a SP8 confocal microscope; photos were taken with 40×. For calculating colocalization, a region of interest in the Cy3 channel or Alexa-647 channel was drawn around JAM-A, ZO-1, or WGA-positive areas. The same region of interest in the Alexa-488 channel was also drawn and the Pearson's correlation coefficient between both channels using ImageJ software was determined ($n = 25$ regions analyzed per condition).

Study Approval. All animal experiments were approved by the Stanford Administrative Panel on Laboratory Animal Care.

Data Availability. All study data are included in the article and/or supporting information.

ACKNOWLEDGMENTS. This work was supported by a Translational Cancer Award from the Stanford Cancer Institute, Stanford's SPARK and Coulter programs, and the Breast Cancer Research program from the Department of Defense grants W81XWH-14-1-0397 (S.L.) and W81XWH-14-1-0398 (S.S.J.), and the National Cancer Institute, USPHS R35CA19735305 (R.L.). F.V.-C. was supported by the American Society of Immunology through a Careers in Immunology fellowship.

1. S. Levy, V. Q. Nguyen, M. L. Andria, S. Takahashi, Structure and membrane topology of TAPA-1. *J. Biol. Chem.* **266**, 14597–14602 (1991).
2. M. E. Hemler, Tetraspanin proteins mediate cellular penetration, invasion, and fusion events and define a novel type of membrane microdomain. *Annu. Rev. Cell Dev. Biol.* **19**, 397–422 (2003).
3. S. Levy, T. Shoham, The tetraspanin web modulates immune-signalling complexes. *Nat. Rev. Immunol.* **5**, 136–148 (2005).
4. B. Zimmerman *et al*., Crystal structure of a full-length human tetraspanin reveals a cholesterol-binding pocket. *Cell* **167**, 1041–1051.e11 (2016).
5. R. Oren, S. Takahashi, C. Doss, R. Levy, S. Levy, TAPA-1, the target of an antiproliferative antibody, defines a new family of transmembrane proteins. *Mol. Cell. Biol.* **10**, 4007–4015 (1990).
6. K. J. Susa, T. C. Seegar, S. C. Blacklow, A. C. Kruse, A dynamic interaction between CD19 and the tetraspanin CD81 controls B cell co-receptor trafficking. *eLife* **9**, e52337 (2020).
7. I. K. Hong *et al*., The tetraspanin CD81 protein increases melanoma cell motility by up-regulating metalloproteinase MT1-MMP expression through the pro-oncogenic Akt-dependent Sp1 activation signaling pathways. *J. Biol. Chem.* **289**, 15691–15704 (2014).
8. N. Mizoshiri *et al*., The tetraspanin CD81 mediates the growth and metastases of human osteosarcoma. *Cell Oncol. (Dordr.)* **42**, 861–871 (2019).
9. Z. C. Uretmen Kagiali *et al*., Systems-level analysis reveals multiple modulators of epithelial-mesenchymal transition and identifies DNAJB4 and CD81 as novel metastasis inducers in breast cancer. *Mol. Cell. Proteomics* **18**, 1756–1771 (2019).
10. F. Vences-Catalán *et al*., Tetraspanin CD81 promotes tumor growth and metastasis by modulating the functions of T regulatory and myeloid-derived suppressor cells. *Cancer Res.* **75**, 4517–4526 (2015).
11. F. Vences-Catalán *et al*., CD81 is a novel immunotherapeutic target for B cell lymphoma. *J. Exp. Med.* **216**, 1497–1508 (2019).
12. F. van Zijl, G. Krupitza, W. Mikulits, Initial steps of metastasis: Cell invasion and endothelial transmigration. *Mutat. Res.* **728**, 23–34 (2011).
13. M. Fedele, L. Cerchia, G. Chiappetta, The epithelial-to-mesenchymal transition in breast cancer: Focus on basal-like carcinomas. *Cancers (Basel)* **9**, E134 (2017).
14. C. Zihni, C. Mills, K. Matter, M. S. Balda, Tight junctions: From simple barriers to multifunctional molecular gates. *Nat. Rev. Mol. Cell Biol.* **17**, 564–580 (2016).
15. S. S. Peddibhotla *et al*., Tetraspanin CD9 links junctional adhesion molecule-A to αvβ3 integrin to mediate basic fibroblast growth factor-specific angiogenic signaling. *Mol. Biol. Cell* **24**, 933–944 (2013).
16. M. U. Naik, T. U. Naik, A. T. Suckow, M. K. Duncan, U. P. Naik, Attenuation of junctional adhesion molecule-A is a contributing factor for breast cancer cell invasion. *Cancer Res.* **68**, 2194–2203 (2008).
17. V. C. Ramani *et al*., Investigating circulating tumor cells and distant metastases in patient-derived orthotopic xenograft models of triple-negative breast cancer. *Breast Cancer Res.* **21**, 98 (2019).
18. H. Zhang *et al*., Patient-derived xenografts of triple-negative breast cancer reproduce molecular features of patient tumors and respond to mTOR inhibition. *Breast Cancer Res.* **16**, R36 (2014).
19. A. M. Razmara *et al*., Tumor shedding and metastatic progression after tumor excision in patient-derived orthotopic xenograft models of triple-negative breast cancer. *Clin. Exp. Metastasis* **37**, 413–424 (2020).
20. T. Hasezaki, T. Yoshima, M. Mattsson, A. Särnefält, K. Takubo, A monoclonal antibody recognizing a new epitope on CD81 inhibits T-cell migration without inducing cytokine production. *J. Biochem.* **167**, 399–409 (2020).
21. F. Vences-Catalán *et al*., A mutation in the human tetraspanin CD81 gene is expressed as a truncated protein but does not enable CD19 maturation and cell surface expression. *J. Clin. Immunol.* **35**, 254–263 (2015).
22. B. Nelson *et al*., Structure-guided combinatorial engineering facilitates affinity and specificity optimization of anti-CD81 antibodies. *J. Mol. Biol.* **430**, 2139–2152 (2018).
23. K. J. Susa, S. Rawson, A. C. Kruse, S. C. Blacklow, Cryo-EM structure of the B cell co-receptor CD19 bound to the tetraspanin CD81. *Science* **371**, 300–305 (2021).
24. W. Oosterheert *et al*., Implications for tetraspanin-enriched microdomain assembly based on structures of CD9 with EWI-F. *Life Sci. Alliance* **3**, e202000883 (2020).
25. M. E. Hemler, Tetraspanin proteins promote multiple cancer stages. *Nat. Rev. Cancer* **14**, 49–60 (2014).
26. M. E. Hemler, Targeting of tetraspanin proteins–Potential benefits and strategies. *Nat. Rev. Drug Discov.* **7**, 747–758 (2008).
27. F. Vences-Catalán *et al*., CD81 as a tumor target. *Biochem. Soc. Trans.* **45**, 531–535 (2017).
28. Y. Zhang, H. Qian, A. Xu, G. Yang, Increased expression of *CD81* is associated with poor prognosis of prostate cancer and increases the progression of prostate cancer cells *in vitro*. *Exp. Ther. Med.* **19**, 755–761 (2020).
29. H. S. Park *et al*., Suppression of CD81 promotes bladder cancer cell invasion through increased matrix metalloproteinase expression via extracellular signal-regulated kinase phosphorylation. *Investig. Clin. Urol.* **60**, 396–404 (2019).
30. K. Pantel, R. H. Brakenhoff, Dissecting the metastatic cascade. *Nat. Rev. Cancer* **4**, 448–456 (2004).
31. X. A. Zhang, A. L. Bontrager, M. E. Hemler, Transmembrane-4 superfamily proteins associate with activated protein kinase C (PKC) and link PKC to specific beta(1) integrins. *J. Biol. Chem.* **276**, 25005–25013 (2001).
32. M. Merzoug-Larabi *et al*., Protein kinase C inhibitor Gö6976 but not Gö6983 induces the reversion of E- to N-cadherin switch and metastatic phenotype in melanoma: Identification of the role of protein kinase D1. *BMC Cancer* **17**, 12 (2017).
33. H. T. Maecker, S. C. Todd, E. C. Kim, S. Levy, Differential expression of murine CD81 highlighted by new anti-mouse CD81 monoclonal antibodies. *Hybridoma* **19**, 15–22 (2000).
34. M. R. Schick, S. Levy, The TAPA-1 molecule is associated on the surface of B cells with HLA-DR molecules. *J. Immunol.* **151**, 4090–4097 (1993).